International Journal of Current Engineering and Technology
E-ISSN 2277 – 4106, P-ISSN 2347 – 5161

Available at http://inpressco.com/category/ijcet

Research Article

The Performance of Hybrid Journal Bearing under Extreme Operating Conditions

Lijesh K.P.†* and Hairsh Hirani†

†Mechanical Department, Indian Institute of Technology Delhi, New Delhi, India

Accepted 28 Jan 2015, Available online 01 Feb 2015, **Vol.5, No.1 (Feb 2015)**

Abstract

Fluid film bearing (FFB) performance is limited to normal operating conditions i.e. at moderate load and rotating speed. At extreme operating conditions like: high load and low speed FFBs do not perform well as contact between journal and bearing-surfaces occurs which results in bearing wear. To deal with these extreme conditions, a hybrid bearing (FFB + Halbach magnetic bearing) is proposed. The load capacity of hybrid bearing is estimated as vector summation of forces exerted due to fluid film lubrication as well as due to magnetic repulsion. In the present manuscript the load capacity of Halbach magnetic (HM) arrangement is estimated by summing the individual forces due to the rotor and stator magnets in axial, radial and perpendicular directions. To exemplify the proposed hybrid bearing arrangement, a case study of sugar mill top half bearing subjected to "high load (>1.5MN) and low rotating speed (5 rpm)" is considered. The results of hybrid bearing show far better performance of hybrid bearing compared to the FFB.

Keywords: *Fluid film bearing, Halbach magnetic bearing, Hybrid Bearing, Sugar mill*

1. Introduction

Fluid film bearings, based on the hydrodynamic mechanism, are known for low friction (Khonsari, Booser, 2001), ultra-low wear (Peterson, Winer, 1980), and high damping (Hirani, Suh, 2005). A well designed fluid film bearing can deal with slight misalignment, fluctuation in speed/load and unexpected dirt. However on increasing load and/or reducing the relative speed, increases the chances of bearing wear. Under "low speed and high load (Muzakkir et al 2013, Hirani, M Verma 2009)" conditions, the performance of FFB decreases drastically and designing an efficient bearing under such operating conditions is really a challenging task. One such practical situation where very low speed and high load occurs is the top half bearing of sugar mills. These bearings are prone to wear and abrade due to metal to metal contact. One of such failed sugar mill bearing is shown in figure 1.

Hydrostatic bearings (Dilip *et al* 1993), which work on external pressurised fluid supplied by pump, can be used for heavy load and low speed conditions, but the blockage of the supply line by the bagasse may result in failure of the system (Dilip *et al* 1993). In addition high initial and running costs avoid the usage of such bearings in sugar mill. Using Active Magnetic Bearing (AMB) is another option available to take the static as well dynamic load, but due to the requirement of controller, high initial as well as running cost (Lijesh, Hirani, 2015, Shankar *et al,* 2006) the economical usage of AMB is not feasible.

Fig.1 Failed fluid film bearing

The other alternative technology available is passive magnetic bearing. Due to the low-cost, durability, and easy availability of high power permanent magnets (i.e. Sm-Co and Nd-Fe-Bo), the use of permanent magnets in number of applications (molecular pumps (Yoichi *et al,* 1992) artificial heart blood pump ((Qian *et al,* 2006) and flywheel (Sahinkaya, 2007) has increased, but the load carrying capacity of magnetic bearings is relatively lesser (Lijesh, Hirani, 2015, Samanta, Hirani, 2007, Muzzakir, 2014). An increase in load capacity can

*Corresponding author: **Lijesh K.P.**

be obtained by using Halbach arrangement (Halbach, 1980, Yukio, 1997, Lee, 2007, Ravaud, Lemarquand, 2009.

A detailed study conducted by Muzakkir *et al,* 2014 on sugar mill bearing concluded that insufficient fluid film (i.e. film unable to prevent the opposing solids to come in the contact) lubrication condition as one of the main reasons of frequent bearing failure. The wear caused by metal to metal contact can be avoided by increasing the rotating speed of the rotor (so that hydrodynamic fluid action is generated), but the increase in the speed will reduce the time for sugarcane to pass through the rollers and hence reduction in the extraction of juice. The mechanical wear can be nullified by decreasing the load supported by FFB. The magnetic repulsion between rotor and stator along with FFB can be used to share the load imposed on fluid film bearing (Lijesh, Hirani, 2014). In the present work an effort has been made to prove that wear in sugar mill FFB can be reduced by hybridizing hydrodynamic action with magnetic repulsion action. The load carrying capacity of hybrid bearing is a vector sum of individual load carrying capacities of FFB and HMB.

The hydrodynamic load carrying capacity of FFB is estimated by using Reynolds equation (Muzakkir *et al*, 2014), while load capacity of HMB is evaluated using 3D Coulombian model for each magnetic arrangement. Iterative loop is being used to estimate the final position of rotor relative to bearing geometric centre.

2. Fluid Film Bearing

The analytical method of (Hirani et al 1997) is fast method to find the hydrodynamic pressure. But the reliability of this method reduces at high eccentricity and low rotational speed. To overcome this problem, finite difference method applied on Reynolds equation (Eq. 1) is used. The Reynolds' equation used to estimate pressure distribution for journal bearing as function of journal speed, film thickness, clearance, and lubricant viscosity in rectangular coordinate is expressed as:

$$\frac{\partial}{\partial x}\left(\frac{h^3}{12\eta}\frac{\partial p}{\partial x}\right)+\frac{\partial}{\partial z}\left(\frac{h^3}{12\eta}\frac{\partial p}{\partial z}\right)=\frac{1}{2}\frac{\partial(U_2-U_1)h}{\partial x}+(V_1-V_2)+\frac{1}{2}\frac{\partial(W_2-W_1)h}{\partial z} \quad (1)$$

Where; p is fluid film pressure in N/mm^2, x is the coordinate in tangential direction and z is the coordinate in axial direction in m.η is the viscosity of the oil Ns/mm^2, U_1, V_1, W_1 are the velocity components of journal and U_2, V_2, W_2 is the velocity component of bearing surface, h is the oil film gap between shaft and bearing surface (h= C(1+ε cos(θ))), ε is eccentricity ratio, ω is angular velocity of shaft in rad/s, and C is radial clearance between journal and bearing in m. If there is no motion other than motion of in x direction, Reynolds equation can be reduced to

$$\frac{\partial}{\partial x}\left(\frac{h^3}{12\eta}\frac{\partial p}{\partial x}\right)+\frac{\partial}{\partial z}\left(\frac{h^3}{12\eta}\frac{\partial p}{\partial z}\right)=\frac{1}{2}U\frac{\partial h}{\partial x} \quad (2)$$

The first step to solve this partial differential equation is to non-dimensionalize it by putting x=Rθ, $\bar{h}=h/C$, $\bar{z}=z/L$ and $\bar{p}=\frac{p}{6\eta\omega\left(\frac{R}{C}\right)^2}$.

$$\frac{\partial}{\partial\theta}\left(\bar{h}^3\frac{\partial\bar{p}}{\partial\theta}\right)+\frac{\partial}{\partial\bar{z}}\left(\bar{h}^3\frac{\partial\bar{p}}{\partial\bar{z}}\right)=\frac{\partial\bar{h}}{\partial\theta} \quad (3)$$

In the above equations θ is coordinate in circumferential direction in radians, R is radius of journal in m. $\bar{h}$, $\bar{z}$, $\bar{p}$ is the non dimensional film thickness, axial distance and pressure of the bearing. By central difference method equation (3) can be written as

$$\bar{p}_{i,j}=\frac{\left(\frac{R}{L}\right)^2\left(\frac{\bar{p}_{i,j+1}+\bar{p}_{i,j-1}}{\Delta\bar{z}^2}\right)+\left(\left(-\frac{3}{2}\frac{\varepsilon\sin\theta}{h\Delta\theta}\right)+\frac{1}{\Delta\theta^2}\right)\bar{p}_{i+1,j}+\left(\left(\frac{3}{2}\frac{\varepsilon\sin\theta}{h\Delta\theta}\right)+\frac{1}{\Delta\theta^2}\right)\bar{p}_{i-1,j}+\left(\frac{R}{L\Delta\bar{z}}\right)^2}{2\left(\frac{1}{\Delta\theta^2}+\left(\frac{R}{L\Delta\bar{z}}\right)^2\right)} \quad (4)$$

$$F_r=\int_{\theta=0}^{2\pi}\int_{o}^{L}p\cos\theta\,dz\,Rd\theta \quad (5)$$

$$F_\theta=\int_{\theta=0}^{2\pi}\int_{o}^{L}p\sin\theta\,dz\,Rd\theta$$

$$F_h=\sqrt{F_r^{\,2}+F_\theta^{\,2}} \quad (6)$$

$$\phi=\tan^{-1}\left(\frac{F_\theta}{F_r}\right) \quad (7)$$

Where, F_h is the hydrodynamic force, equation (6) is solved in MATLAB software by applying necessary boundary condition and having convergence criteria between two iterative values as kept as < 10^{-6}. Attitude angle is found by using (7).

3 Mathematical Modelling for Hybrid Bearing

To develop hybrid bearing, Halbach arrangement (shown in figure 2) consists of axial (as shown in figure 3a), radial (as shown in figure 3b) and perpendicular polarized magnets (shown in figure 3c) has been used. In such an arrangement, the magnetic field increases on one side and equivalent reduction in magnetic field on the other side occurs.

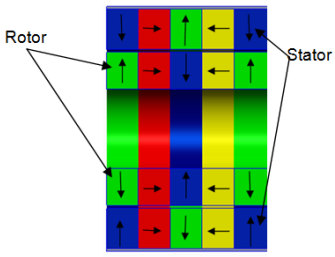

Fig.2 Halbach Arrangement

The total load carrying capacity of Halbach arrangement ($F_{r,HAL}$) is given by:

$F_{r,HAL}$= Σ [Σ(Radial polarized)+ Σ(Axial polarized)+ Σ(Perpendicular polarized)]

$$F_{r,RMD} = \sum\left(\sum_{j=1}^{k} F_{r,z,j} + \sum_{j=1}^{m} F_{r,r,j} + \sum_{j=1}^{n} F_{r,p,j}\right) \quad (8)$$

Where 'k' is the number of segments of axially, 'm' is number of radially polarized and 'n' is number of perpendicular polarized magnets in Halbach configuration. (Yonnet, 1978) proved that for an identical bearing, the load carrying capacity between two radially polarized magnets remains same as load capacity between two axially polarized magnets. Hence, a separate formulation for radial polarized magnets is not required and the equation (8) can be modified as:

$$F_{r,HAL} = \sum\left(\sum_{j=1}^{k+m} F_{r,z,j} + \sum_{j=1}^{n} F_{r,p,j}\right) \quad (9)$$

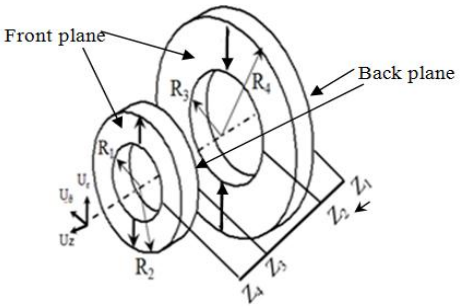

(a) Axial polarized bearing

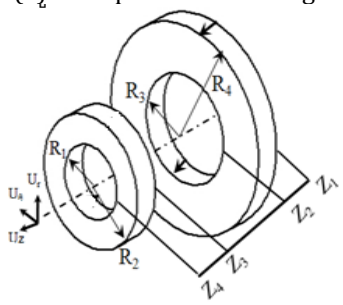

(b) Radial polarized bearing

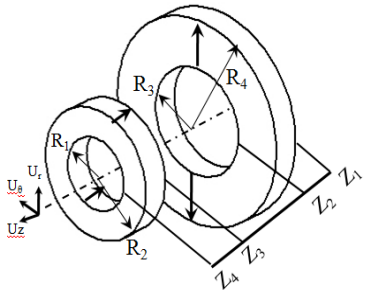

(c) Perpendicular polarized bearing

Fig. 3 stator and rotor magnets in different magnetic bearing arrangements

3.1 Axially Polarized Magnet

According to Coulombian model, axially polarized magnets is represented by two charged planes located on the upper and bottom surfaces of the ring. The charge distribution in the front plane of ring permanent magnet is +σ* and in the back plane is -σ* as shown in figures 3(a) and 4(a). σ_1^* and σ_2^* are the charge distributions of the stator and rotor magnets respectively. The radial force between two axially polarized full ring magnets is given by equation (10) and the detailed derivation of this equation is provided in [13].

$F_{r,z}=(Br_1Br_2/4\pi\mu_0)(R(z_a)+R(z_a+H-B)-R(z_a+H)-R(z_a-B))$ (10)

Where R(α) is given by :

$$R(z_a) = \int_0^{2\pi}\int_0^{2\pi}\int_{R_3}^{R_4}\int_{R_1}^{R_2} \left[\frac{(e + r_{12}\cos(\theta) - r_{34}\cos(\theta'))r_{12}r_{34}}{\left(\begin{array}{l} r_{12}^{\,2} + r_{34}^{\,2} + e^2 - 2r_{12}r_{34}\cos(\theta-\theta') \\ +2e(r_{12}\cos(\theta) - r_{34}\cos(\theta')) + (z_a)^2 \end{array}\right)^{1.5}}\right] dr_{12}dr_{34}d\theta d\theta' \quad (11)$$

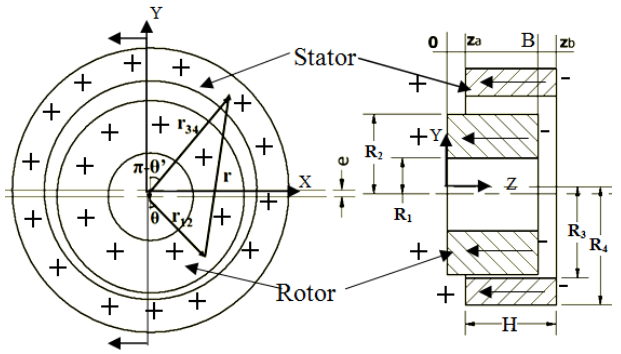

(a) Front View (b) Sectional Side View

Fig.4 Coordinates of Magnetic bearing

Where 'e' is the eccentricity between the rotor and stator magnet, R_1 and R_2 is the inner and outer radius of the rotor magnet and R_3 and R_4 is inner and outer radius of the stator magnet as shown in figure 4(a). H is the axial length of the stator magnet and B is the axial length of rotor magnet. z_a is the axial offset between the rotor and stator magnet as shown in figure 4(b). 'θ' is the angle subtend by the stator magnet, for a full ring stator magnet 'θ' varies from 0 and 2π and for bottom half magnet θ' varies from – π/2 to π/2. The value of z_a is replaced by (z_a+H-B, z_a+H, z_a-B) in equation (10) for evaluating $F_{r,z}$ in equation (11).The four integration in equation (11) four is reduced to three integration (equation (12)) for fast evaluation and the equation can be easily integrated in MATLAB using "triplequad" function.

$$R(z_a) = \int_0^{2\pi}\int_0^{2\pi}\int_{R_3}^{R_4} I(r_{34},\theta,\theta')dr_{34}d\theta d\theta' \quad (12)$$

Where;

$A_1(z_a)$	$\left(e+r_{34}\cos(\theta')\right)\ r_{34}$
$B_1(z_a)$	$r_{34}\cos(\theta)$
$C_1(z_a)$	$\left(e^2+{r_{34}}^2+(z_a)^2-2r_{34}e\cos(\theta')\right)$
$D_1(z_a)$	$\left(e\cos(\theta)-2r_{34}\cos(\theta-\theta')\right)$
$F(z_a)$	$\left(\frac{A_1(4C_1+2D_1R_2)}{\left(\left(4C_1-{D_1}^2\right)\left((R_2)^2+D_1R_2+C_1\right)^{0.5}\right)}-\frac{A_1(4C_1+2D_1R_1)}{\left(\left(4C_1-{D_1}^2\right)\left({R_1}^2+D_1R_1+C_1\right)^{0.5}\right)}\right)$
$G(z_a)$	$B_1\log\left(\frac{D_1}{2}+R_2+\left({R_2}^2+D_1R_2+C_1\right)^{0.5}\right)-\left(\frac{B_1\left(R_2\left(C_1-0.5{D_1}^2\right)-C_1D_1 0.5\right)}{\left(C_1-0.25{D_1}^2\right)\left({R_2}^2+D_1R_2+C_1\right)^{0.5}}\right)-B_1\log\left(\frac{D_1}{2}+R_1+\left({R_1}^2+D_1R_1+C_1\right)^{0.5}\right)-\left(\frac{B_1\left(R_1\left(C_1-0.5{D_1}^2\right)-C_1D_1 0.5\right)}{\left(C_1-0.25{D_1}^2\right)\left({R_1}^2+D_1R_1+C_1\right)^{0.5}}\right)$
$I(r_2,\theta,\theta')$	$\left(\begin{array}{l}F(z_a)+F(z_a+H)-F(z_a+H-B)-F(z_a-B)\\+G(z_a)+G(z_a+H)-G(z_a+H-B)-G(z_a-H)\end{array}\right)$

Equation (12) provides the value of $A(z_a)$ of equation (10). Values of $A(z_a+H-B)$, $A(z_a+H)$, $A(z_a-B)$ are calculated by replacing the z_a by (z_a+H-B, z_a+H, z_a-B) in equation (12).

3.2 Perpendicular Polarized Magnet

The radial force between the two rings in a perpendicular polarized magnetic bearing ($F_{r,p}$) is given in equation (13).

$$F_{r,p}=Br_1Br_2/4\pi\mu_0(A(z_a,R_1)-A(z_a+H,R_1)-(z_a,R_2)+A(z_a+H,R_2)) \quad (13)$$

Where;

$$A(z_a,R_1)=\int_0^{2\pi}\int_0^{2\pi}\int_{R_3}^{B}\int^{R_4}\frac{\left(e+R_1\cos(\theta)-r_{34}\cos(\theta')\right)R_1r_{34}}{\left(\begin{array}{l}{R_1}^2+{r_{34}}^2+e^2-2R_1r_{34}\cos(\theta-\theta')+\\2eR_1\left(R_1\cos(\theta)-r_{34}\cos(\theta')\right)+(z_a-z_{34})^2\end{array}\right)}dr_{34}dz_{34}d\theta d\theta'$$

Similarly equation (14) can be reduced to three integrations by:

$$A(r_3,r_1)=\int_0^{2\pi}\int_0^{2\pi}\int_{R_3}^{R_4}I(r_{34},\theta,\theta')dr_{34}d\theta d\theta' \quad (14)$$

$I(r_{34},\theta,\theta')$	$C_2(z_a,R_1)-C_2(z_a+b,R_1)-C_2(z_a,R_2)+C_2(z_a+H,R_2)$
$A_2(z_a,R_1)$	$\left(e-R_{34}\cos(\theta')+R_1\cos(\theta)\right)\ R_{34}R_1$
$B_2(z_a,R_1)$	$\left(\begin{array}{l}e^2+{R_1}^2+{R_{34}}^2-2eR_{34}\cos(\theta')+\\2R_1e\cos(\theta)-2R_{34}R_1\cos(\theta-\theta')\end{array}\right)$
$C_2(z_a,R_1)$	$\frac{A_2(z_a)}{\left(B_2\left(B_2+(z_a)^2\right)^{0.5}\right)}-\frac{A_2(H-z_a)}{\left(B_2\left(B_2+(H-z_a)^2\right)^{0.5}\right)}$

The total radial force for Halbach arrangement ($F_{r,HAL}$) is estimated by summing the individual force by the magnets in axial polarization (equations 10 and 12) and perpendicular polarization (equations 13 and 14). The total radial force for Halbach arrangement is given by equation (9).

3.3 Hybridization of Magnetic and Hydrodynamic Bearings

To estimate the load carrying capacity of hybrid bearing, vector sum of journal and magnetic forces needs to be evaluated. For calculating the combined effect of FFB and HMB forces, the following procedure is followed:

1) Initial guess of eccentricity ratio is given as input.
2) For the assumed eccentricity ratio, the HMB force is calculated for given outer radius and axial length of the bearing using equations (1).
3) Hydrodynamic and altitude angle are calculated for the given radial clearance and rotational speed of the rotor.
4) Calculate the vector sum of the FFB and HMB. If load is lesser than the applied load, choose new value of eccentricity ratio.
5) Estimate the eccentricity ratio using Newton Raphson method (equation (15)) and repeat steps 2 to 4 for finding the eccentricity ratio for which the sum of hydrodynamic and magnetic force is equal to the total external load acting on the bearing. If the sum of load carrying capacity by HMB and FFB is lesser than applied load, the bearing will be operating in mixed lubrication condition. There is need to redesign the hybrid bearing.

$$e(n+1)=e(n)+\frac{f(n)}{f'(n)} \quad (15)$$

4. Sugar Mill Case Study

In sugar mill, for extracting the juice from sugar cane, sugarcanes are squeezed between four rollers (Top roller, Feed roller, Discharge roller and Underfeed roller as shown in figures 5(a) and 5(b)) along with one underfeed roller. Underfeed roller is just for feeding the sugarcanes, and it doesn't play any role in squeezing of sugarcanes. The three roller mill arrangement with underfeed roller consists of cast iron shells mounted on heavy steel shafts and are arranged to rotate in opposite direction from other. Pressure is applied on the top roller using hydraulic arrangement for squeezing the sugar cane and due to this reason the failure of the bearing in the top roller is more frequent. The bearing consists of two parts: (i) Bottom half bearing made of bronze metal is stationary (shown in figure 6) and (ii) the top half of the bearing is made of silver metal and moves along with hydraulic arrangement. The dimension (275 mm radius, 600 mm in axial length and radial clearance is 250μm) of the

top sugar mill bearing; the rotating speed of the roller as 5 rpm and load on the top roller as 1.8 MN have been considered.

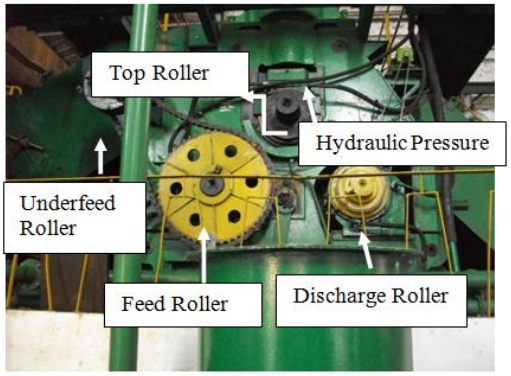

(a) Front view of the sugar mill rollers

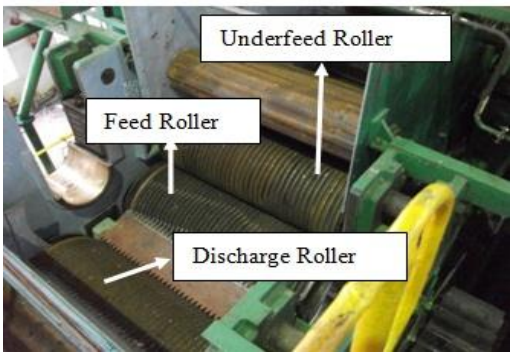

(b) Top view of the rollers without top rollers

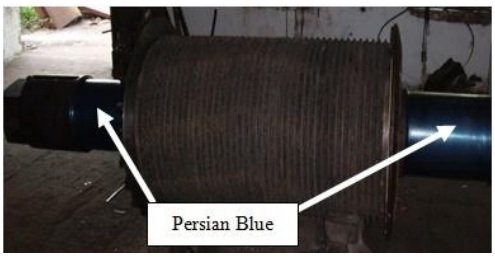

(c) Top Roller

Fig. 5 Sugar mill rollers

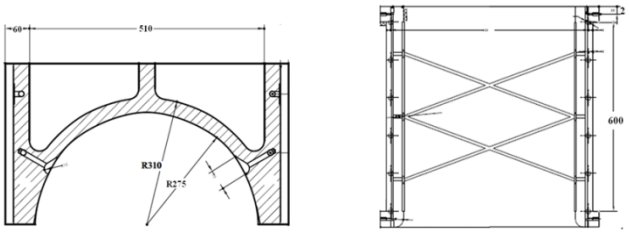

(a) Front view (b) Top view

Fig.6 Sugar mill bearing

The numerical analysis was carried out for fluid film and hybrid bearings. The upper limit of eccentricity ratio equal to 0.983 was fixed. To estimate the exact journal location, equation (15) has been used. The initial guess of eccentricity ratio was considered to be 0.4 and increment in the load with the estimated eccentricity ratio using equation (15) is shown in figure 7. The estimated load for FFB comes out to be 1.0577MN, while for the hybrid bearing it is 2.0647MN. This means on using the hybrid bearing in sugar mills eliminate the wear of the bearing (Load capacity >1.8N).

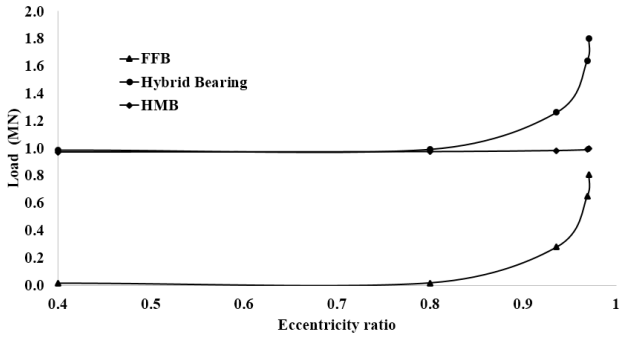

Fig. 7 Load vs Eccentricity ration

Conclusion

A study on FFB operating in extreme conditions (low speed and high load) has been carried out. To reduce the wear in the FFB, hybrid bearing was proposed. The total load by the HMB was estimated by summing the load carried by the axial and perpendicular polarized arrangements. To check the feasibility of the hybrid bearing a case study of sugar mill top bottom bearing was considered. Theoretical analysis was performed for the sugar mill bearing. Based on the current study, the following conclusions can be made:

1) HMB load carrying capacity is not affected by the change in eccentricity ratio.
2) FFBs and hybrid bearings are greatly affected by the change in eccentricity ratio
3) Using hybrid bearing, higher load carrying capacity can be achieved.

References

M.M. Khonsari, E.R. Booser, (2001), Applied Tribology, Bearing design and lubrication, New York, *JohnWiley & Sons Inc*.

M.B. Peterson, W.O. Winer, (1980), "Wear control handbook". New York: *ASME*.

H. Hirani, N.P. Suh, (2005), Journal bearing design using multiobjective genetic algorithm and axiomatic design approaches, *Tribol Int*, vol.38, pp.481–491.

S M Muzakkir, H Hirani, G D Thakre, (2013), Lubricant for Heavily-Loaded Slow Speed Journal Bearing, *Tribology Transactions*, vol.56,no.6, pp. 1060-1068

H Hirani and M Verma, (2009), Tribological study of elastomeric bearings of marine shaft system, *Tribology International*, vol.42, no.2, pp.378-390.

K. Dilip, Chaudhuri, J.S. Andrew, D. S. James, (1993), Friction and oxidative wear of 440C ball bearing steels under high

load and extreme bulk temperatures, *Wear*, vol.160, pp.37-50.

K .P. Lijesh, H Hirani, (2015), Optimization of Eight Pole Radial Active Magnetic Bearing, *ASME, Journal of Tribology*, vol.137, no.2, available online.

S Shankar, Sandeep and H Hirani, (2006), Active Magnetic Bearing, *Indian Journal of Tribology*, pp 15-25.

K. Yoichi S. Kanemistu, S. Yuji, (1992), Turbo molecular pump, *US Patent Number* 5152679.

K.X. Qian, P. Zeng, W.M. Ru, H.Y. Yuan, (2006), New concepts and new design of permanent maglev rotary artificial heart blood pumps, *Medical Engineering & Physics*, vol.28, pp.383–388.

M.N. Sahinkaya, A.H.G. Abulrub, P.S. Keogh, C.R. Burrows, (2007), Multiple Sliding and Rolling Contact Dynamics for a Flexible Rotor/Magnetic Bearing System, *IEEE/ASME Trans. Mechatronics*, vol.12, no.2, pp.179–189.

K P Lijesh, H Hirani, (2015), Development of Analytical Equations for Design and Optimization of Axially Polarized Radial Passive Magnetic Bearing", *ASME, Journal of Tribology*, vol.137, no.1, pp.111031-111039

H. Hirani, P. Samanta, (2007), Hybrid (Hydrodynamic + Permanent Magnetic) Journal Bearings, Proc. *Institute Mech. Engineers., Part J, Journal of Engineering Tribology*, vol.221,no.8,pp. 881-891.

S.M. Muzzakir, K.P. Lijesh, H Hirani, (2014), Tribological Failure Analysis of a Heavily-Loaded Slow Speed Hybrid Journal Bearing, *Engineering Failure Analysis*, vol.40, pp.97–113.

K. Halbach, (1980), Design of permanent multipole magnets with oriented rare earth cobalt material, *Nuclear Instruments and Methods*, vol.169, pp.1-10.

H. Yukio, Y. Shizuka, H. Toshiro, T. Yoji, (1997), Using the Halbach Magnet Array to Develop an Ultrahigh-speed Spindle Motor for Machine Tools, *IEEE Industry Applications Society Annual Meeting New Orleans*, pp. 5-9.

M.G. Lee, S.Q. Lee and D.G. Gweon, (2004), Analysis of Halbach magnet array and its application to linear motor, *Mechatronics*, vol.14, pp.115–128.

R. Ravaud, G. Lemarquand, (2010), Halbach Structures for Permanent Magnets Bearings, *Progress In Electromagnetics Research M*, vol.14, pp. 263-277.

K .P. Lijesh, H Hirani, (2014), Stiffness and damping coefficients for rubber mounted hybrid bearing, Lubrication Science, vol.26, no.5, pp.301-314.

S.M. Muzakkir, H. Hirani, G.D. Thakre, M.R. Tyagi, (2011), Tribological failure analysis of journal bearings used in sugar mills, *Engineering Failure Analysis*, vol.18, pp.2093–2103.

H. Hirani, T.V.V.L.N. Rao, K. Athre, S. Biswas, (1997), Rapid performance evaluation of journal bearings, *Tribol Int*, vol.30, no.11, pp.825–834.

J.P. Yonnet, (1978), Passive magnetic bearings with permanent magnets, *IEEE Trans. Magn.*,vol.14, pp. 803-805.